

Supporting Information

Mechanistic Insight into H₂-Mediated Ni Surface Diffusion and Deposition to form the Branched Ni Nanocrystals: A Theoretical Study

Yan Li,¹ Ning Liu,^{2} Chengna Dai,² Ruinian Xu,² Bin Wu,²*

Gangqiang Yu,² Biaohua Chen²

¹State Key Laboratory of Chemical Resource Engineering, Beijing University of Chemical Technology, Beijing, 100029, China.

²College of Environmental and Energy Engineering, Beijing University of Technology, Beijing, 100124, China.

*Corresponding author:

liuning@bjut.edu.cn (N. Liu)

Table of Content

Table S1a. Calculated activation barriers (ΔE^*_{diff} , eV), Gibbs formation energies (ΔG_{form} , eV), diffusion coefficients (D , cm²·s⁻¹), apparent activation barriers (ΔE^*_{app} , eV), pre-exponential factors (k_0 , cm²·s⁻¹) of atomic Ni on Ni(111) surfaces at 423 K.S1

Table S1b. Calculated activation barriers (ΔE^*_{diff} , eV), Gibbs formation energies (ΔG_{form} , eV), diffusion coefficients (D , cm²·s⁻¹), apparent activation barriers (ΔE^*_{app} , eV), pre-exponential factors (k_0 , cm²·s⁻¹) of atomic Ni on Ni(100) surfaces at 423 K.S2

Table S1c. Calculated activation barriers (ΔE^*_{diff} , eV), Gibbs formation energies (ΔG_{form} , eV), diffusion coefficients (D , $\text{cm}^2\cdot\text{s}^{-1}$), apparent activation barriers (ΔE^*_{app} , eV), pre-exponential factors (k_0 , $\text{cm}^2\cdot\text{s}^{-1}$) of atomic Ni on Ni(110) surfaces at 423 K.	S3
Table S2. Optimized models of Ni(111), Ni(100) and Ni(110) [p(4×4)] with surface H coverages 0, 1, 1.5, 1.75 and 2 ML; and subsurface H coverage of 1ML.	S4
Figure S1. Atomic Ni surface diffusions from 3-fold hollow site to the neighboring 3-fold hollow site over Ni(111) under different diffusion conditions.	S5
Figure S2. Atomic Ni surface diffusions form 4-fold hollow site to another neighboring 4-fold hollow site over Ni(100) under different diffusion conditions.	S6
Figure S3. Atomic Ni surface diffusions from vertical 4-fold hollow site to the neighboring 4-fold hollow site over Ni(110) under different diffusion conditions.	S7
Figure S4. Surface diffusion coefficient of Ni diffusion to form dimer over (a) Ni(111); (b) Ni(100); (c) Ni(110) under different conditions of ■ clean surface, ● subsurface H of 1 ML, ▼ surface H of 1 ML, and maximum surface H coverage ▲ of 1.5 ML for Ni(111), 1.75 ML for Ni(100), and 2 ML for Ni(110).	S8
Figure S5. Ni surface diffusion over Ni(111) of [p(6×6)] after formation of the NiH complex based on DFT.	S9
Figure S6. Calculated partial DOS for adatom Ni on Ni(111) under different conditions.	S10
Figure S7. Calculated partial DOS for adatom Ni on Ni(100) under different conditions.	S11
Figure S8. Calculated partial DOS for adatom Ni on Ni(110) under different conditions.	S12
Verification of structure stability of the model systems under high hydrogen concentration environments	S13
Figure S9 H atom surface diffusions over Ni(111), Ni(100) and Ni(110).	S14
Atomic Ni Deposition Rate Measured by AIMD	S15

Table S1a Calculated activation barriers (ΔE^*_{diff} , eV), Gibbs formation energies (ΔG_{form} , eV), diffusion coefficients (D_s , $\text{cm}^2\cdot\text{s}^{-1}$), Apparent activation barriers (ΔE^*_{app} , eV), pre-exponential factors (k_0 , $\text{cm}^2\cdot\text{s}^{-1}$) of atomic Ni on Ni(111) surfaces at 423 K.

Ni(111)	E_{diff} / eV	$\Delta G_{form} / \text{eV}$	$D_s / \text{cm}^2 \text{ s}^{-1}$	E_{app} / eV	$k_0 / \text{cm}^2 \text{ S}^{-1}$
Clean Surface	0.35	0.50	6.03×10^{-5}	1.44	1.1×10^{13}
Subsurface 1ML	0.20	0.77	2.62×10^{-6}	1.54	6.0×10^{12}
Surface 1ML	0.58	1.59	1.24×10^{-19}	2.82	5.81×10^{14}
Surface 1.5ML	0.38	2.05	2.19×10^{-22}	3.20	3.96×10^{16}

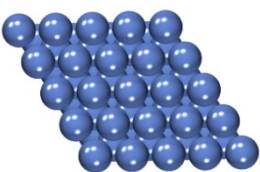
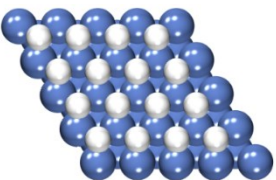
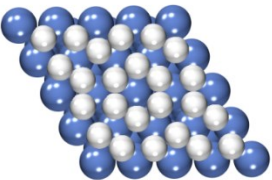
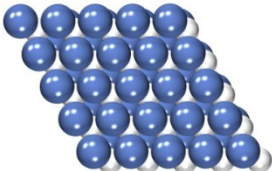
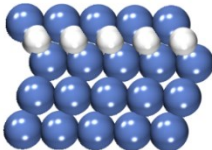
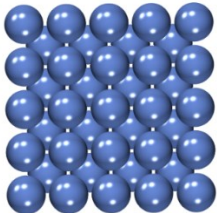
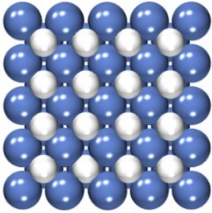
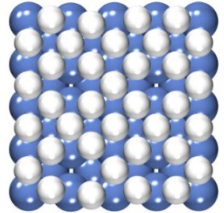
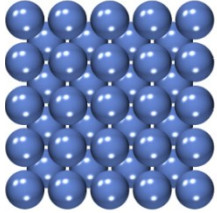
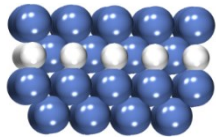
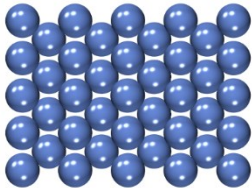
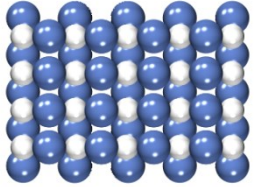
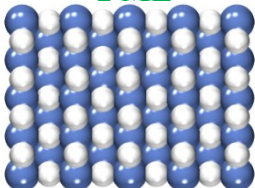
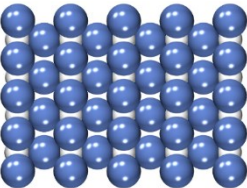
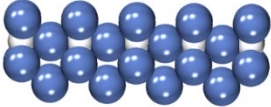
Table S1b Calculated activation barriers (ΔE^*_{diff} , eV), Gibbs formation energies (ΔG_{form} , eV), diffusion coefficients (D_s , $\text{cm}^2\cdot\text{s}^{-1}$), Apparent activation barriers (ΔE^*_{app} , eV), pre-exponential factors (k_0 , $\text{cm}^2\cdot\text{s}^{-1}$) of atomic Ni on Ni(100) surfaces at 423 K.

Ni(100)	E_{diff} / eV	$\Delta G_{form} / \text{eV}$	$D_s / \text{cm}^2 \text{ s}^{-1}$	E_{app} / eV	$k_0 / \text{cm}^2 \text{ S}^{-1}$
Clean Surface	1.03	-0.76	6.58×10^{-5}	3.07	4.66×10^{32}
Subsurface 1ML	0.96	-1.13	32.4	2.84	4.22×10^{35}
Surface 1ML	0.39	0.77	2.18×10^{-17}	3.77	3.50×10^{28}
Surface 1.75ML	0.57	0.96	1.17×10^{-21}	3.63	6.74×10^{22}

Table S1c Calculated activation barriers (ΔE^*_{diff} , eV), Gibbs formation energies (ΔG_{form} , eV), diffusion coefficients (D_s , $\text{cm}^2 \cdot \text{s}^{-1}$), Apparent activation barriers (ΔE^*_{app} , eV), pre-exponential factors (k_0 , $\text{cm}^2 \cdot \text{s}^{-1}$) of atomic Ni on Ni(110) surfaces at 423 K.

Ni(110)	E_{diff} / eV	$\Delta G_{form} / \text{eV}$	$D_s / \text{cm}^2 \text{ s}^{-1}$	E_{app} / eV	$k_0 / \text{cm}^2 \text{ S}^{-1}$
Clean Surface	0.68	-0.67	2.35×10^{-4}	1.11	5.78×10^9
Subsurface 1ML	0.56	-1.02	2.63×10^2	1.16	2.85×10^{16}
Surface 1ML	0.59	-0.98	1.67×10^2	0.87	5.88×10^{12}
Surface 2 ML	0.95	-0.57	3.45×10^{-9}	1.53	8.71×10^9

Table S2 Optimized models of Ni(111), Ni(100) and Ni(110) [p(4×4)] with surface H coverages 0, 1, 1.5, 1.75 and 2 ML; and subsurface H coverage of 1ML.

Surface Orientation	Slab Model	H Surface Coverage of 1ML	H Surface Coverage of 1.5, 1.75 and 2ML	H Subsurface Coverage of 1ML (Top view)	H Subsurface Coverage of 1ML (Side view)
^a Ni(111)			1.5ML 		
^b Ni(100)			1.75 ML 		
^c Ni(110)			2 ML 		

^a The atomic H occupies the FCC site under the θ_H of 1 ML; in addition to FCC site the additional H atoms occupy the HCP site under the θ_H of 1.5 ML; subsurface H atoms occupy the FCC site under coverage of 1 ML.

^b The atomic H occupies the 4 fold hollow site under the θ_H of 1 ML; in addition to 4 fold hollow site the additional H atoms occupy the bridge site under the θ_H of 1.75 ML; subsurface H atoms occupy the 4 fold hollow site under coverage of 1 ML.

^c The atomic H occupies the 4 fold hollow site under the θ_H of 1 ML; in addition to 4 fold hollow site the additional H atoms occupy the bridge site under the θ_H of 2.0 ML; subsurface H atoms occupy the 4 fold hollow site under coverage of 1 ML.

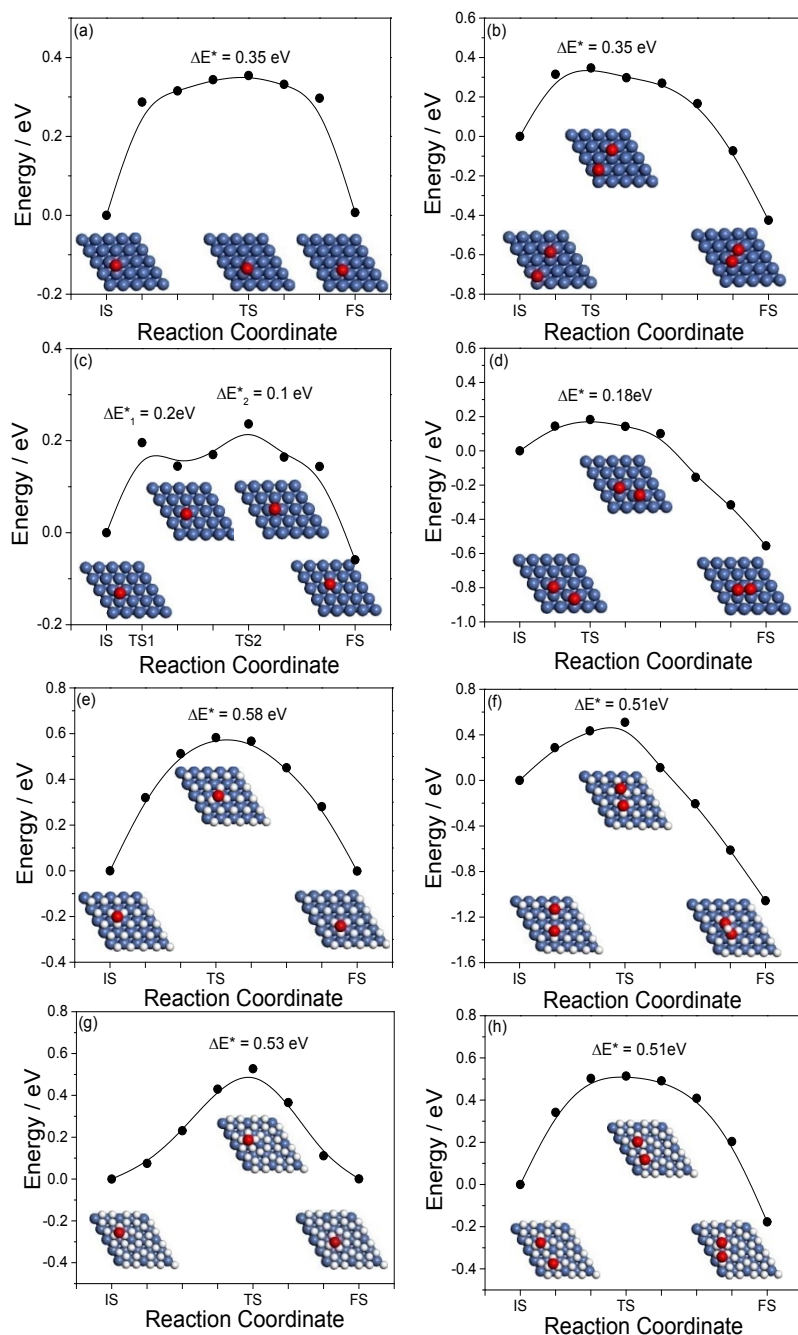


Figure S1 Atomic Ni surface diffusions from 3-fold hollow site to the neighboring 3-fold hollow site over Ni(111) under different diffusion conditions: (a) single Ni diffusion and (b) forming Ni dimer over clean slab(from FCC to HCP); (c) single Ni diffusion and (d) forming Ni dimer under subsurface H of 1ML(from FCC to HCP); (e) single Ni diffusion and (f) forming Ni dimer under surface H of 1ML(from HCP to HCP); (g) single Ni diffusion and (h) forming Ni dimer under surface H of 1.5 ML(from HCP to HCP).

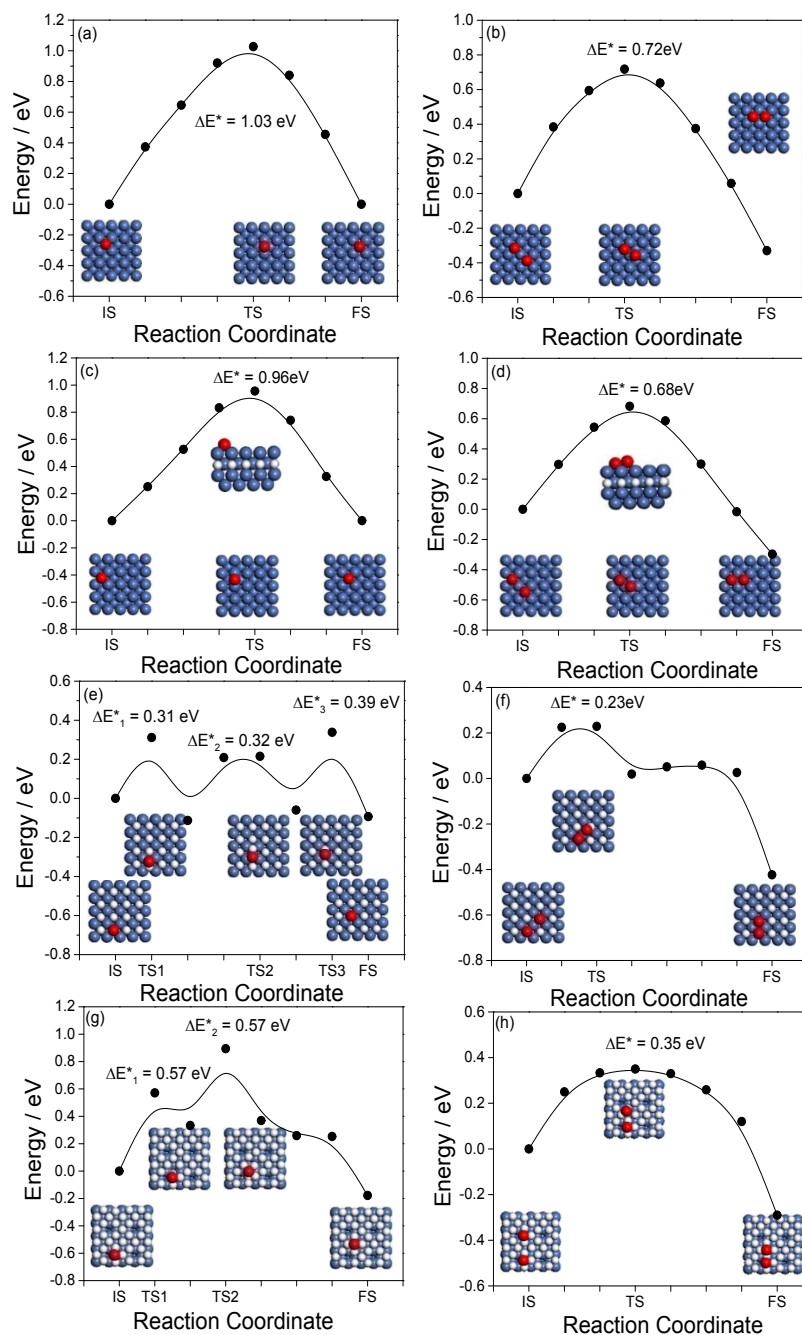


Figure S2 Atomic Ni surface diffusions from 4-fold hollow site to another neighboring 4-fold hollow site over Ni(100) under different diffusion conditions: (a) single Ni diffusion and (b) forming Ni dimer over clean slab; (c) single Ni diffusion and (d) forming Ni dimer under subsurface H of 1ML; (e) single Ni diffusion and (f) forming Ni dimer under surface H of 1ML; (g) single Ni diffusion and (h) forming Ni dimer under surface H of 1.75 ML.

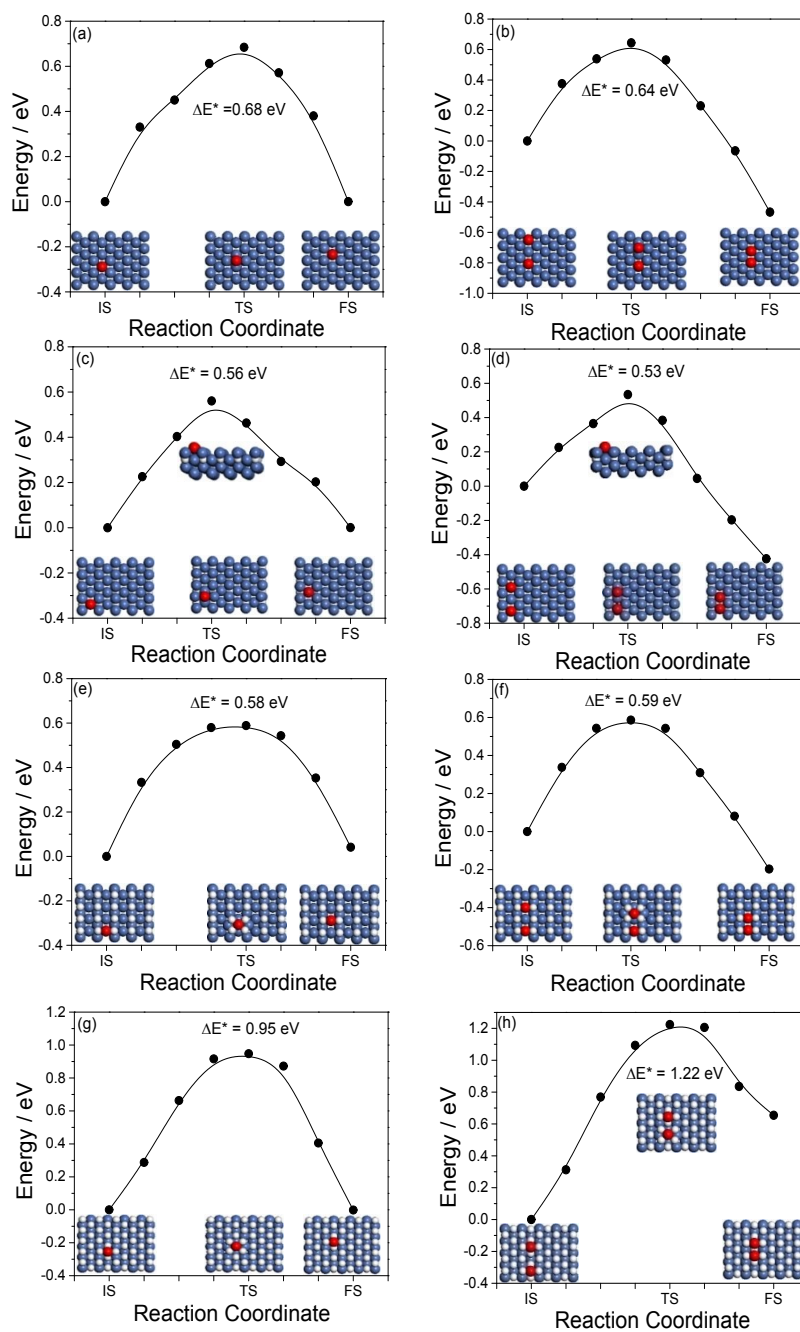


Figure S3 Atomic Ni surface diffusions from vertical 4-fold hollow site to the neighboring 4-fold hollow site over Ni(110) under different diffusion conditions: (a) single Ni diffusion and (b) forming Ni dimer over clean slab; (c) single Ni diffusion and (d) forming Ni dimer under subsurface H of 1ML; (e) single Ni diffusion and (f) forming Ni dimer under surface H of 1ML; (g) single Ni diffusion and (h) forming Ni dimer under surface H of 2 ML.

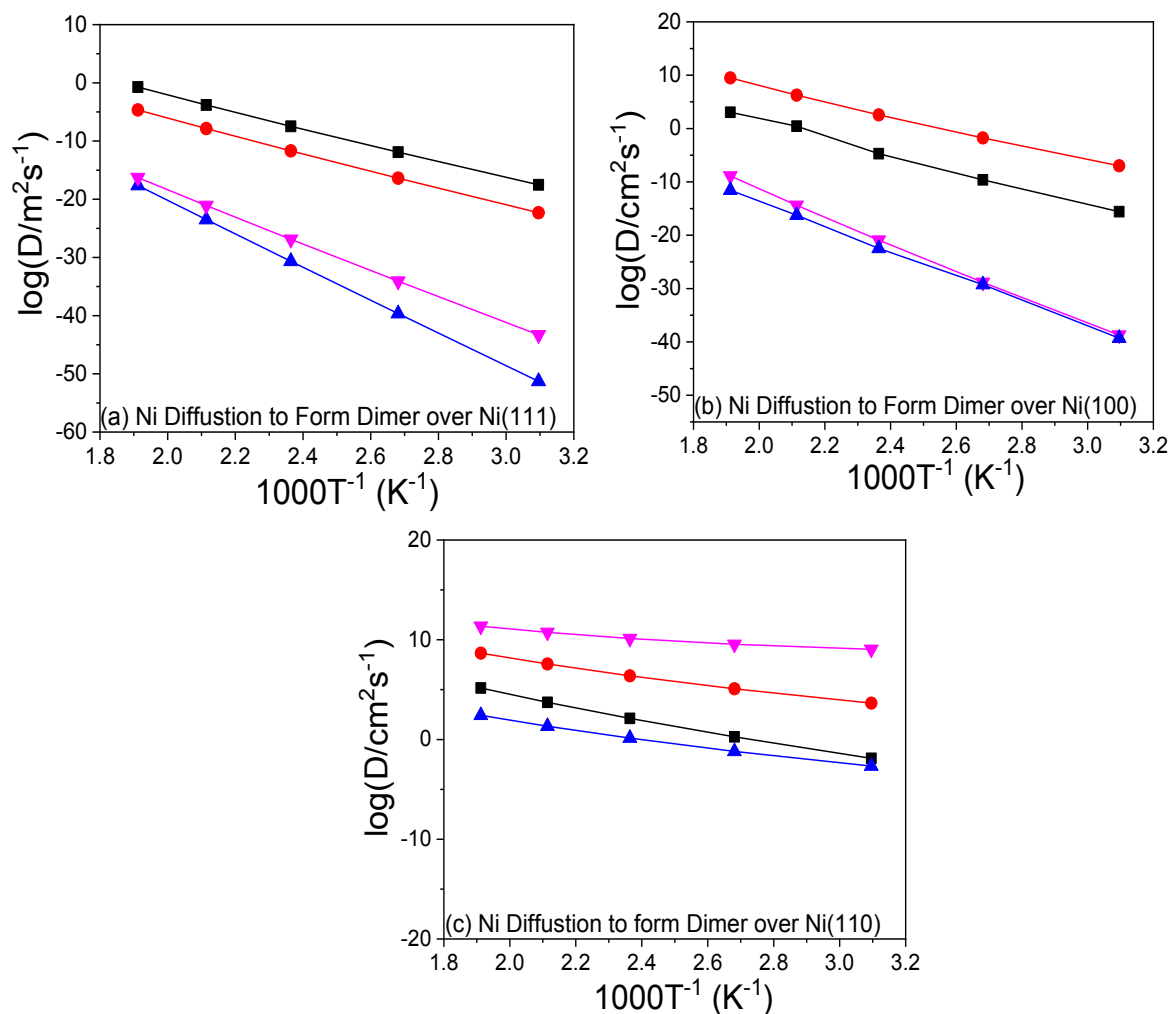


Figure S4 Surface diffusion coefficient of Ni diffusion to form dimer over (a) Ni(111); (b) Ni(100); (c) Ni(110) under different conditions of ■ clean surface, ● subsurface H of 1 ML, ▼ surface H of 1 ML, and maximum surface H coverage ▲ of 1.5 ML for Ni(111), 1.75 ML for Ni(100), and 2 ML for Ni(110).

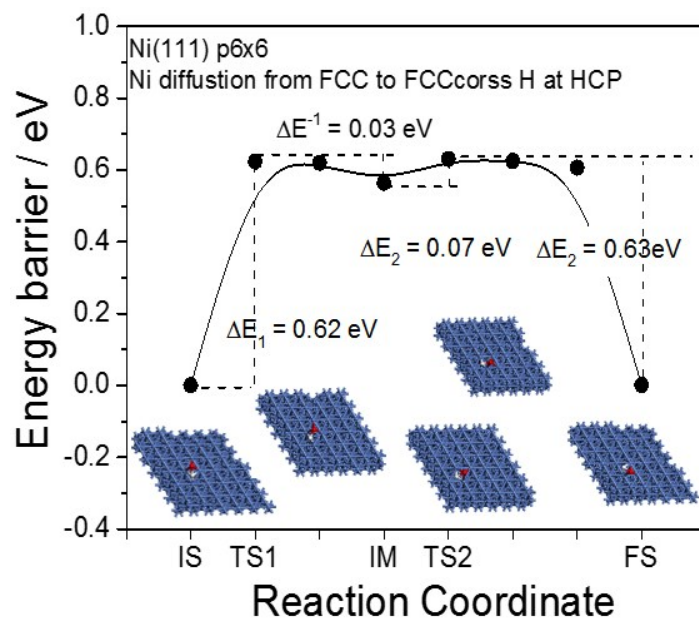


Fig. S5 Ni surface diffusion over Ni(111) of [p(6×6)] after formation of the NiH complex based on DFT; white atom represents H and red atom represents the diffusing atom Ni.

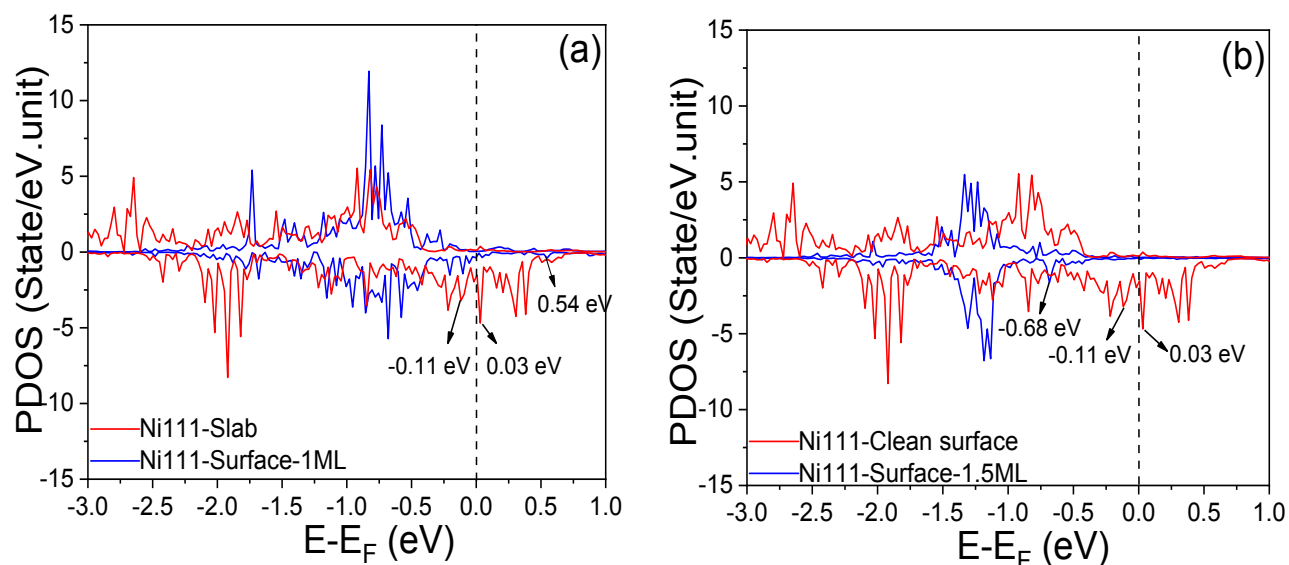


Figure S6 Calculated partial DOS for adatom Ni on Ni(111) under different conditions: (a) clean facet (red line) and surface covered by 1 ML of H (blue line); (b) clean facet (red line) and surface covered by 1.5 ML of H (blue line).

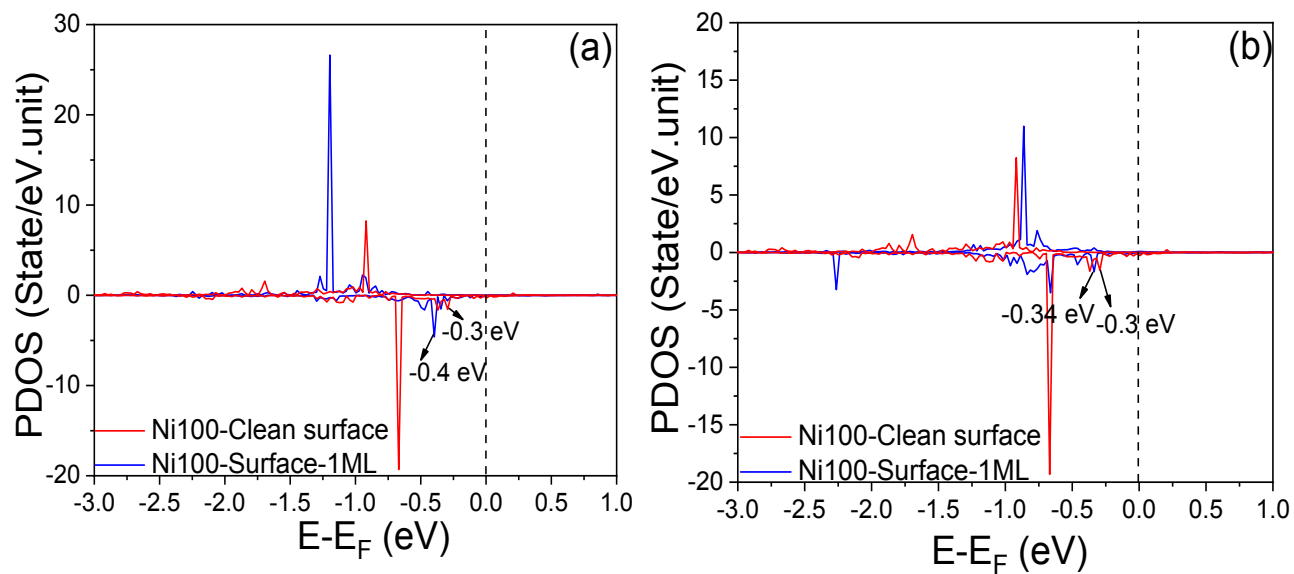


Figure S7 Calculated partial DOS for adatom Ni on Ni(100) under different conditions: (a) clean facet (red line) and surface covered by 1 ML of H (blue line); (b) clean facet (red line) and surface covered by 1.75 ML of H (blue line).

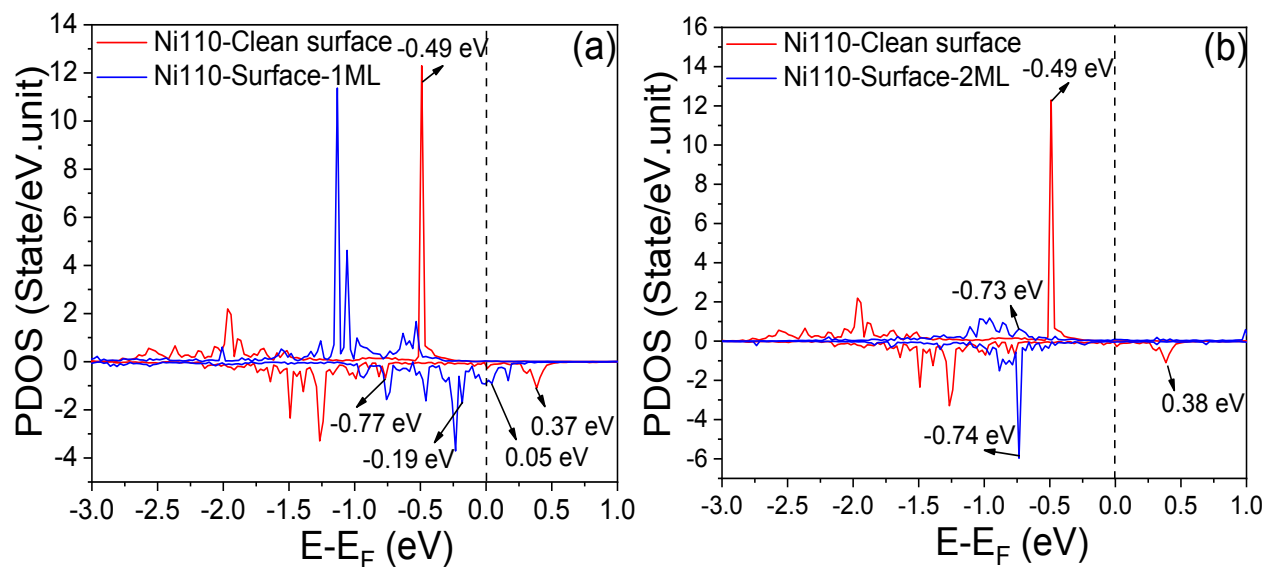


Figure S8 Calculated partial DOS for adatom Ni on Ni(110) under different conditions: (a) clean facet (red line) and surface covered by 1 ML of H (blue line); (b) clean facet (red line) and surface covered by 2 ML of H (blue line).

Verification of structure stability of the model systems under high hydrogen concentration environments

Firstly, we investigate atomic H surface diffusions over the clean facets of Ni(111), Ni(100) and Ni(110). It can be found that the H surface diffusions can readily occur over the clean facet of Ni slaps by overcoming relative lower energy barrier ($\Delta E = 0.22 - 0.4$ eV, see Figs. S9a-S9c).

Then, we further conduct the ab initio molecular dynamics (AIMD) simulations by taking the surface H coverages of 1 and 1.5 ML into account over the Ni(111) (taken as the examples) to investigate the surface H diffusions on the structure stability. Herein, it should be noted that the H surface diffusions on monolayer surface H coverage or multiple-layer-surface H coverage are out of the scope of the DFT simulations. As can be seen (Supporting Information Movie #3 and Movie #4), there are no surface H diffusions during the 1 ps NVT simulations ($T = 453$ K); and the Ni(111) kept well structure stabilities under both the 1 and 1.5 ML surface H coverages, which can be majorly related to the steric hindrance of the adsorbed surface H. Therefore, the structure stability of the model systems under a whole monolayer subsurface H coverage or multiple-layer-surface H coverage can be verified based on the AIMD simulations.

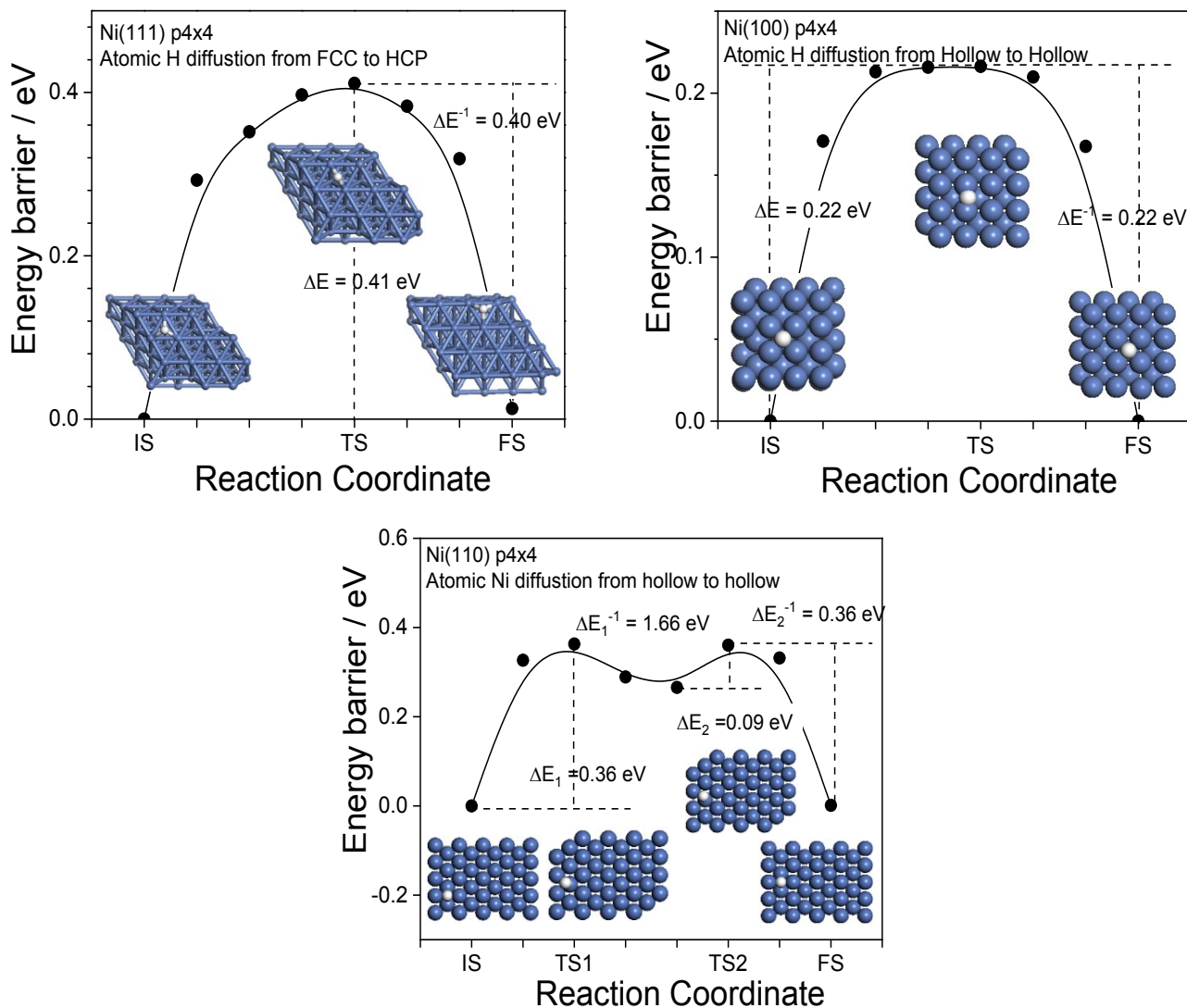


Fig. S9 H atom surface diffusions over (a) Ni(111) (from FCC to HCP); (b) Ni(100) from the 4 fold Hollow to the neighboring 4 fold Hollow site; (c) Ni(110) from the 4 fold Hollow to the neighboring 4 fold Hollow site.

Atomic Ni Deposition Rate Measured by AIMD

1) Atomic Ni Deposition on Ni(111).

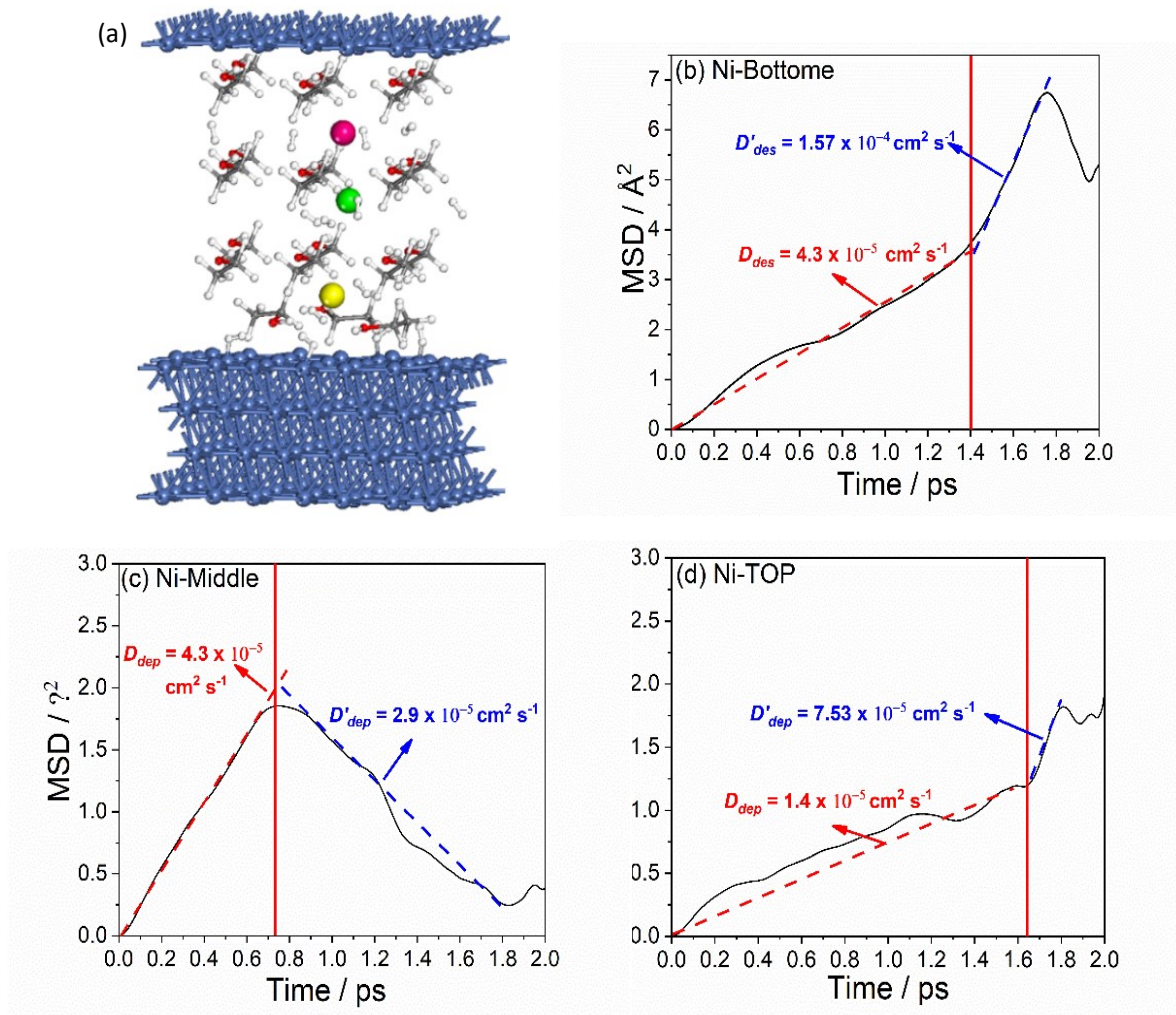


Fig. S10 (a) constructed Ni(111) models, p(4×6) of four layers, utilized in AIMD simulations containing 21 C₂H₅OH, 15 H₂, and three Ni atoms; the Ni atoms located at different heights (normal to the surface) were marked as pink (top Ni), green (middle Ni) and yellow (bottom Ni);MSD for AIMD trajectory of atom Ni on Ni(111) p(4 × 6) with linear fitting: (b) bottom Ni; (c) middle Ni; (d) top Ni.

In order to illustrate the kinetic role of H₂ played during Ni deposition, we further simulated the Ni deposition in a solution condition, containing 21 C₂H₅OH, 15 H₂, and 3 Ni atoms, based on AIMD over Ni(111) surface slab. The constructed model was shown in Fig. S10a, and the whole AIMD simulation process can be visualized in a video supplied in the Supporting Information. Initially, the H₂ molecule added on the surface of Ni(111) (top layer of Fig. S10a)

could be readily dissociated into the adsorbed H atoms. During this process little influence from liquid C₂H₅OH was observed, being mainly related to the much stronger adsorption ability of the dissociated atomic H on the Ni(111) surface.¹⁷ However, when the C₂H₅OH interacted with the bottom layer of Ni(111) slab, being in the absence of surface H₂, we did also observe the subtraction of two H atoms from the C₂H₅OH producing the adsorbed H atoms and liquid acetaldehyde (C₂H₄O). This finding will be further discussed later.

(a) Bottom Ni Deposition. The bottom Ni deposition onto the surface (top layer) of Ni(111) can be divided into two processes: (i) deposition in C₂H₅OH liquid phase being surrounded by two dispersed H₂ molecules; (ii) with an additional participation of the surface atomic H after the Ni deposition close to the top layer of Ni(111). A cooperation effect between the H₂ molecule and surface atomic H was clearly observed, which greatly increased the bottom Ni desorption rate. As verified by Fig. S10b, displaying the mean squared displacement (MSD) for the AIMD trajectory of the bottom Ni, the curve slope, being corresponding to $6 D_{dep}$, became much steeper as $1.75 > t > 1.4$ ps with respect to that of $t < 1.4$ ps. This resulted in the derived D_{dep} being increased from 4.3×10^{-5} ($t < 1.4$ ps) to 1.57×10^{-4} ($1.75 > t > 1.4$ ps) cm² s⁻¹. As noted, the Ni deposition at $t < 1.4$ ps was corresponding to the first deposition scenario, wherein only the surrounded H₂ molecule and liquid C₂H₅OH influenced the Ni deposition; while the surrounded H₂ molecules and surface atomic H cooperatively influenced Ni deposition at $1.75 > t > 1.4$ ps. In addition to that, it is worth noticing that the curve slope became negative at $1.95 > t > 1.75$ ps, which was corresponding to the reverse diffusion of the bottom Ni, from Ni(111) surface toward the liquid phase. However, due to the strong adsorption effect with Ni(111) surface slab, the deposited atomic Ni was hard to escape from the surface of Ni(111).

(b) Middle Ni Deposition. Being different from that of bottom Ni, the middle Ni deposition was only influenced by the surrounded H₂ molecules (two H₂ molecules) and liquid C₂H₅OH. The surface atomic H was not taken into account, because the middle Ni could not be deposited close to the surface of Ni(111) at the investigated time range of 2ps.

As shown in Fig. S10c, two types of deposition constants (D_{dep}) can be derived: the first one with the value of 4.3×10^{-5} cm² s⁻¹ was corresponding to the middle Ni deposition toward the top layer of Ni(111) (displaying the positive curve slope); while, the other one with the value of 2.9×10^{-5} m² s⁻¹ was related to the middle Ni deposition toward to bottom layer of Ni(111) (displaying the negative curve slope). As noted, these values were comparable to that of the bottom Ni

obtained at $t < 1.4$ ps (4.3×10^{-5} cm² s⁻¹), however, were much lower than that derived at $1.75 > t > 1.4$ ps (1.57×10^{-4} cm² s⁻¹) of bottom Ni. This finding revealed that the cooperation effect between the surrounded H₂ molecule (in the liquid phase) and the surface atomic H executed much higher promotion effect than that of the sole H₂ molecule during Ni deposition process, which thereby resulted in much higher D_{des} values.

(c) Top Ni Deposition. The top Ni deposition was toward the bottom layer of Ni(111) (see the AIMD Video of Supporting Information). As shown in Fig. S10d, two types of the deposition constants can be derived from the MSD profile of the top Ni. The first D_{dep} with the value of 1.4×10^{-5} cm² s⁻¹ ($t < 1.65$ ps) was corresponding to the top Ni deposition in the liquid phase mainly influenced by the C₂H₅OH. The dispersed H₂ molecules being located far from the top Ni in the liquid phase exhibited small influences on the Ni deposition. The derived D_{dep} of the top Ni ($D_{dep} = 1.4 \times 10^{-5}$ cm² s⁻¹) was lower than those of bottom Ni (4.3×10^{-5} cm² s⁻¹, $t < 1.4$ ps) and middle Ni (4.3×10^{-5} and 2.9×10^{-5} cm² s⁻¹), wherein the Ni deposition were influenced by both the surrounded H₂ molecule and the liquid C₂H₅OH. This finding gives us a clue that the surrounded H₂ molecule (in the liquid phase) could also promote Ni depositions, in comparison to that of sole C₂H₅OH.

At $1.8 > t > 1.6$ ps, a big promotion of the D_{des} (from 1.4×10^{-5} to 7.53×10^{-5} cm² s⁻¹) was found for the top Ni in Fig. 4d. Detailed analyzing the AIMD video of the Supporting Information, it was realized that the promotion effect of D_{des} originated from the surface atomic H being subtracted from the C₂H₅OH on the bottom layer of Ni(111). The subtracted atomic H on Ni(111) bottom layer could favor the top Ni deposition through the Ni-H interaction. Therefore, the strong promotion effect of the surface atomic H can be well illustrated during top Ni deposition onto the bottom layer of Ni(111). As noted, the MSD profile of Fig. 4d at $t > 1.8$ ps was attributed to the surface motion of the top Ni atom on the bottom layer of Ni(111).

2). Atomic Ni Deposition on Ni(110).

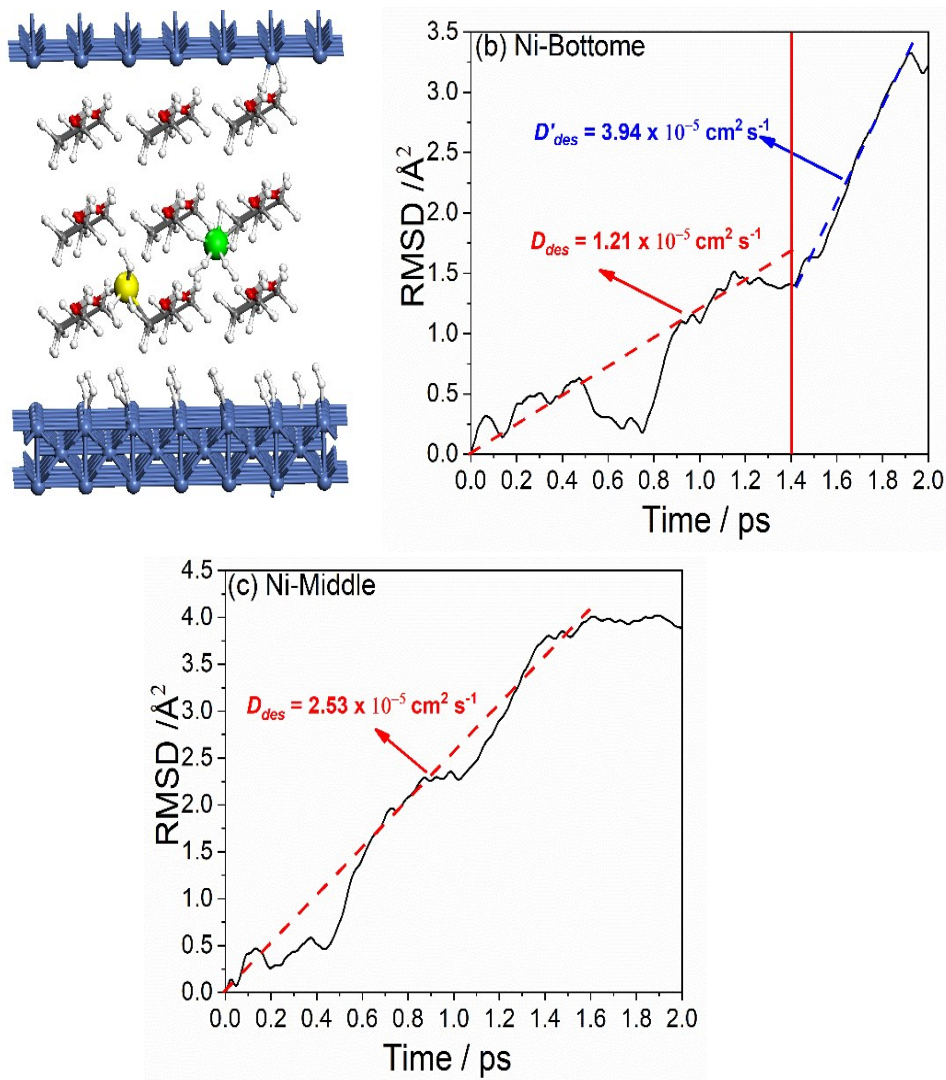


Fig. S11 (a) constructed Ni(110) models, $p(3 \times 6)$ of four layers, utilized in AIMD simulations containing 27 $\text{C}_2\text{H}_5\text{OH}$, 16 H_2 , and two Ni atoms; the Ni atoms located at different heights were marked as green (middle Ni) and yellow (bottom Ni); MSD for AIMD trajectory of atom Ni on Ni(110) $p(3 \times 6)$ with linear fitting: (b) bottom Ni; (c) middle Ni.